

## Supporting Information

# Convective Self-Assembly of 2D Non-Close-Packed Binary Au Nanoparticle Array with Tunable Optical Properties

Changchang Xing, Dilong Liu,\* Jinxing Chen, Yulong Fan, Fei Zhou, Keerat Kaur, Weiping Cai, Yue Li\*

**Changchang Xing** – Key Lab of Materials physics, Institute of Solid State Physics, HFIPS, Chinese Academy of Sciences, Hefei 230031, P. R. China; University of Science and Technology of China, Hefei 230026, P. R. China

**Dilong Liu** - Key Lab of Materials physics, Institute of Solid State Physics, HFIPS, Chinese Academy of Sciences, Hefei 230031, P. R. China; E-mail: dliu@issp.ac.cn

**Jinxing Chen** - Department of Chemistry, University of California, Riverside, CA 92521, United States

**Yulong Fan**- Department of Materials Science and Engineering, City University of Hong Kong, Kowloon, Hong Kong, 999077, P.R. China

**Fei Zhou**- School of Electronic Engineering and Intelligentization, Dongguan University of Technology, Dongguan, 523808, P.R. China

**Keerat Kaur** - Department of Chemistry, University of California, Riverside, CA 92521, United States

**Weiping Cai** - Key Lab of Materials physics, Institute of Solid State Physics, HFIPS, Chinese Academy of Sciences, Hefei 230031, P. R. China

**Yue Li** - Key Lab of Materials physics, Institute of Solid State Physics, HFIPS, Chinese Academy of Sciences, Hefei 230031, P. R. China; E-mail: yueli@issp.ac.cn

### This PDF file includes:

Clausius-Clapeyron Equation

The enhancement factor (EF) calculation

Table S1

Figs. S1 to S17

References

**Clausius–Clapeyron Equation:**<sup>51</sup>

$$\ln P = \frac{-\Delta H_{vap}}{R} \left( \frac{1}{T} \right) + C \quad (1)$$

Where,  $\ln P$  is the natural logarithm of the vapor pressure,  $\Delta H_{vap}$  is the enthalpy of vaporization,  $R$  is the universal gas constant [8.314 J/(mol•K)],  $T$  is the temperature in kelvins, and  $C$  is the y-intercept constant.

The evaporation enthalpies of water, ethanol and ethylene Glycol are summarized in Table S1. It is noteworthy that these three types of solvents have significantly different saturated vapor pressures and surface tensions. To exclude the influence of surface tension of solvent on the substrate, we measured the contact angles of these three solvents on the substrates of 2D NCP unary Au nanoparticle array before and after the hydrophilic treatment by UV-ozone cleaning, as shown in Figure S16. Although these three solvents have total different contact angles on the substrate before hydrophilic treatment, all of them show ultra-small contact angles ( $< 5^\circ$  for water, and  $0^\circ$  for EG and ethanol) on the substrate after the hydrophilic treatment. These results indicate the substrates after the treatment are super-hydrophilic, and thus the surface tension difference of these three solvents should have a negligible effect on the self-assembly process.

**The enhancement factor (EF) calculation**

The enhancement factor (EF) of the 2D NCP binary Au NP arrays was calculated by the equation of:<sup>52</sup>

$$EF = (I_{SERS} / N_{SERS}) / (I_{normal} / N_{normal}) \quad (2)$$

Where,  $I_{SERS}$  is the intensity of  $1080 \text{ cm}^{-1}$  peak acquired from 4-ATP molecules with a concentration of  $10^{-6} \text{ M}$  on the binary Au NP array.  $I_{normal}$  is the intensity of  $1080 \text{ cm}^{-1}$  peak obtained from 4-ATP molecules with a concentration of  $10^{-1} \text{ M}$  on Si substrate.  $N_{SERS}$  and  $N_{normal}$  are the number of the 4-ATP molecules absorbed on the binary Au NP array and the Si substrate, respectively. Herein,  $I_{SERS}$  and  $I_{normal}$  were measured from the SERS spectra. The  $N_{ads}/N_{normal}$  was estimated from the concentration ratio of 4-ATP molecules dropped on the 2D binary array and Si substrate. Here, the  $I_{SERS}$  and  $I_{normal}$  are 21970.70 and 345.13, respectively, as

shown in Figure S17, and the  $N_{ads}/N_{normal}$  we used in here is  $10^5$ , and thus the EF of 2D binary array is ca.  $6.37 \times 10^6$ .

**Table S1.** Comparison of the parameter properties of water, ethylene glycol and ethanol.<sup>53</sup>

|                               | Water        | Ethylene Glycol | Ethanol      |
|-------------------------------|--------------|-----------------|--------------|
| Density (g/mL)                | 1.0          | 1.1             | 0.8          |
| Surface Tension (mN/m)        | 72.06        | 44.98           | 21.91        |
| Saturated Vapor Pressure (Pa) | 3169 (25 °C) | 266 (60 °C)     | 8000 (25 °C) |
| $\Delta H_{vap}$ (kJ/mol)     | 40.65        | 65.6            | 38.6         |

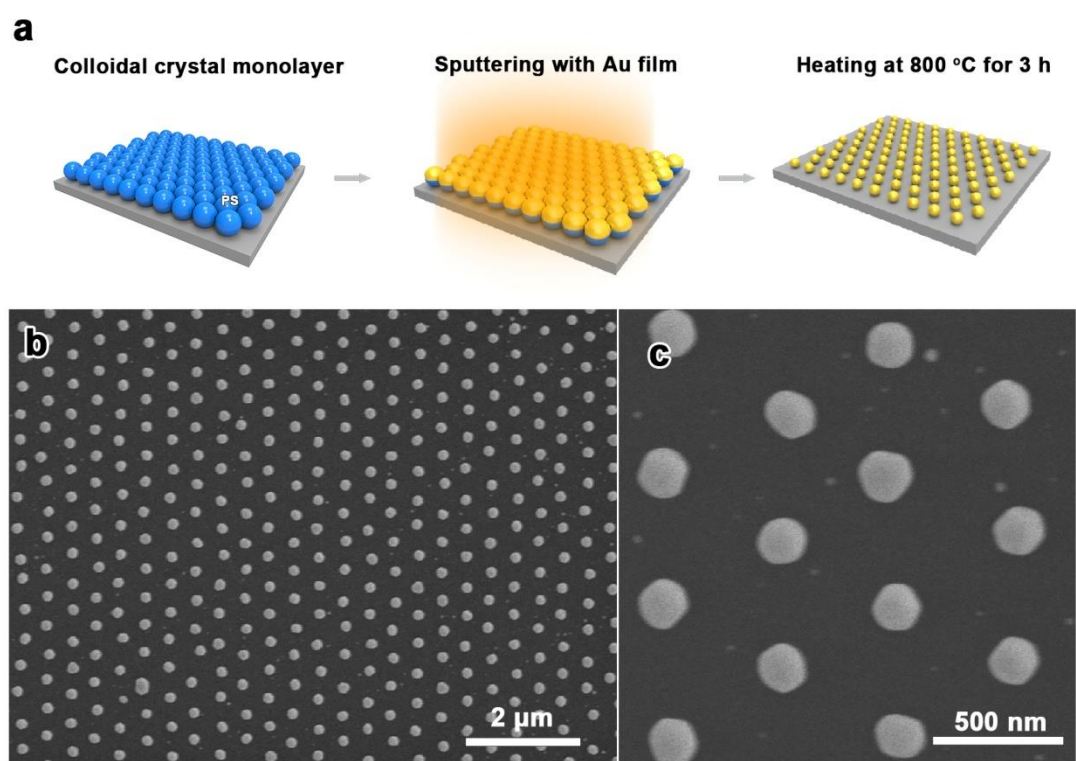


**Figure S1.** (a) Schematic illustration of the fabrication of 2D NCP Au nanoparticle array. (b, c) The typical SEM images of 2D NCP unary Au nanoparticle array used as the self-assembly template.

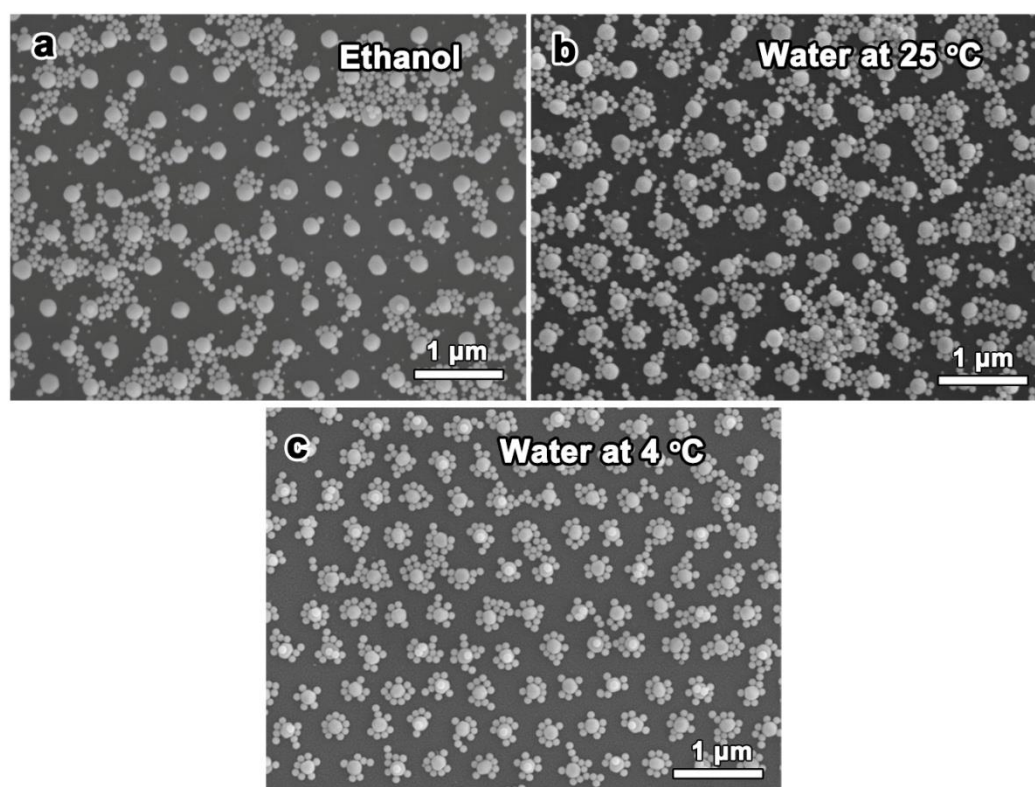


**Figure S2.** The SEM images of the colloidal Au NPs assembled on the NCP unary Au NP array by using different carrying solvents at a given temperature, which are ethanol solvent evaporated at 25 °C (a), water evaporated at 25 °C (b) and 4 °C (c).

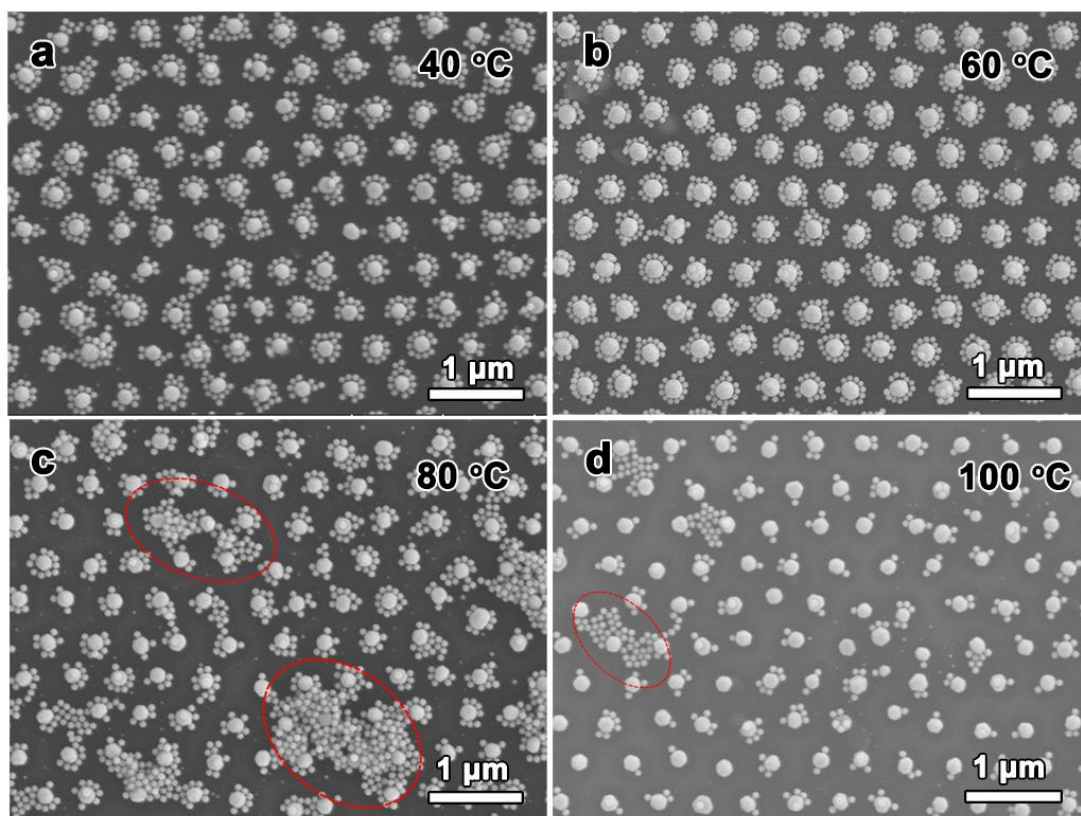


**Figure S3.** Typical SEM images of the arrays after the carrying EG solvent evaporated at 40 °C

(a), 60 °C (b), 80 °C (c), and 100 °C (d).

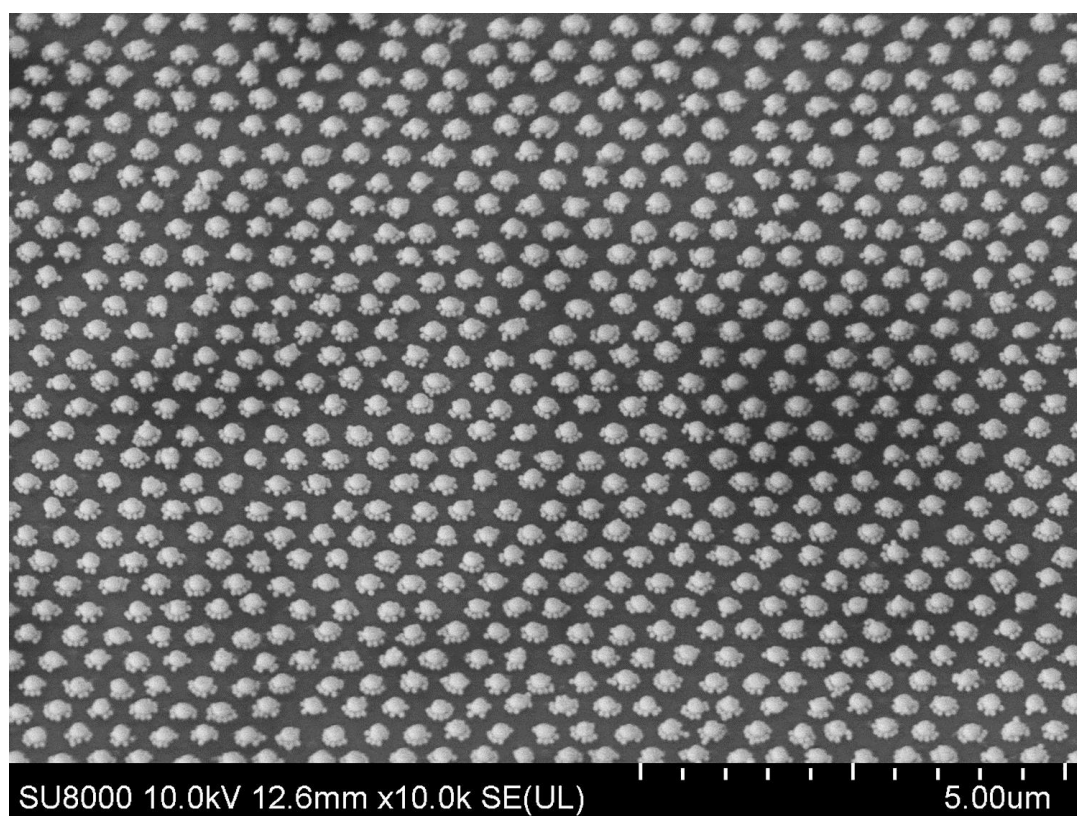


**Figure S4.** The SEM image of 2D NCP binary Au NP array with core-satellite-structured unit in a 45° tilted-view.

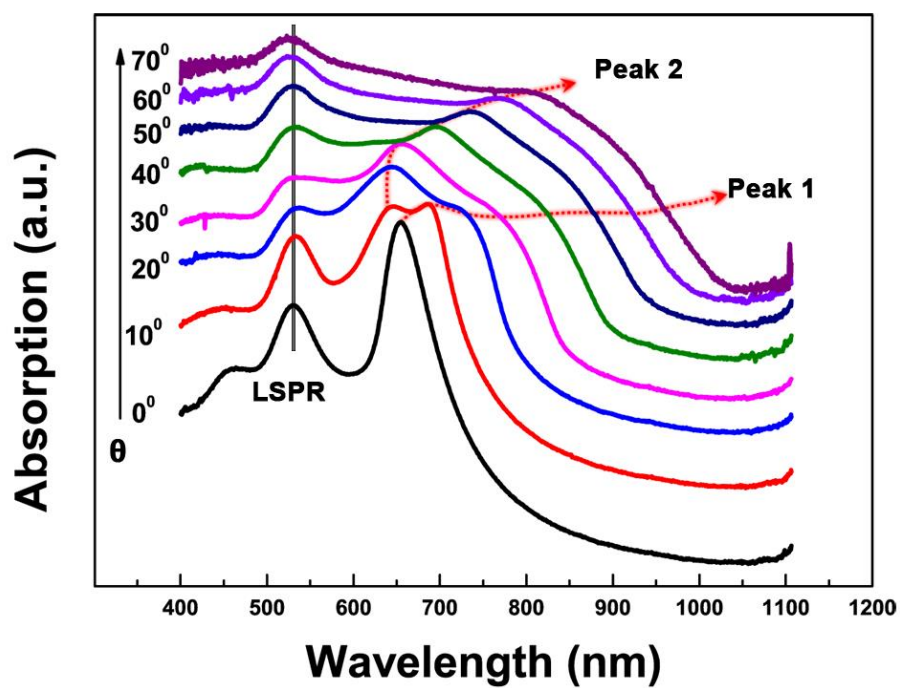


**Figure S5.** The extinction spectra of 2D NCP unary Au nanoparticle array measured at different incident angles ( $\theta$ ). Note:  $\theta$  is the angle between the incident light and the normal direction of 2D array. The diffraction peak is dramatically red-shifted with increasing the angle, while the LSPR peak does not change.



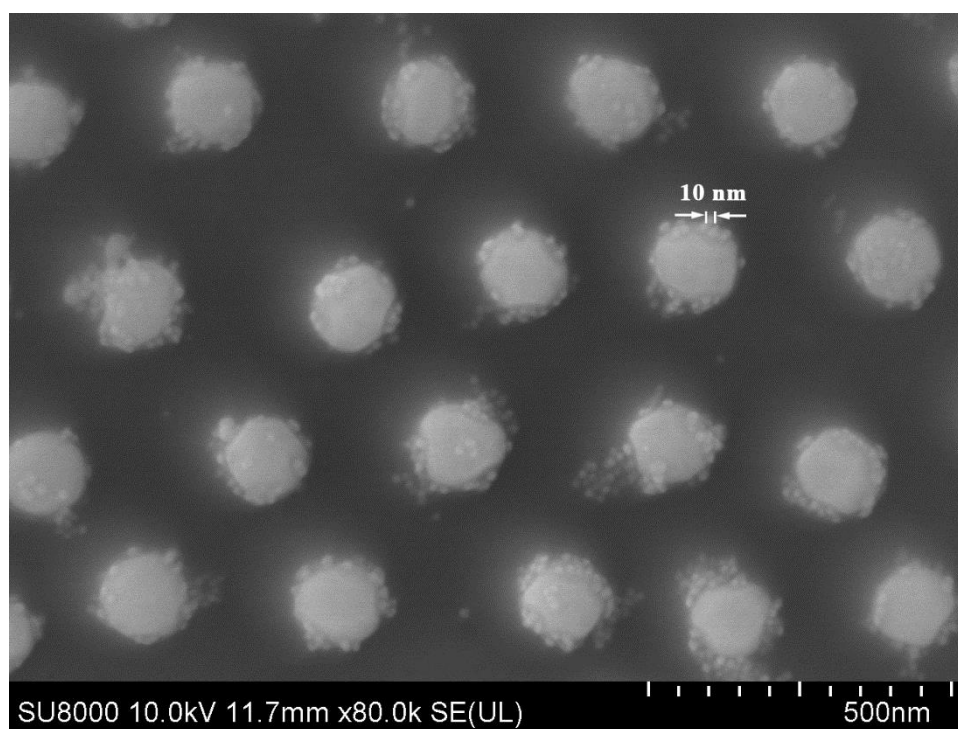


**Figure S6.** The SEM image of 2D NCP binary Au NP array with the satellite Au NP size of 10 nm.

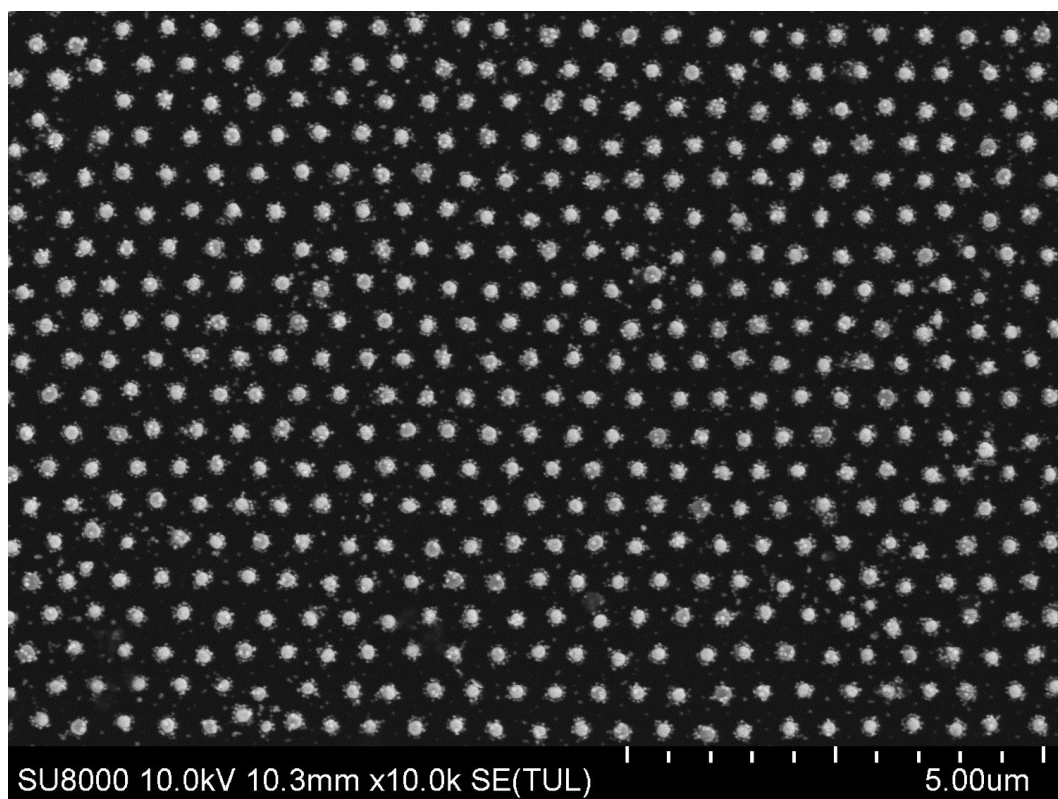


**Figure S7.** The SEM image of 2D NCP binary Au NP array with the satellite Au NP size of 25 nm.

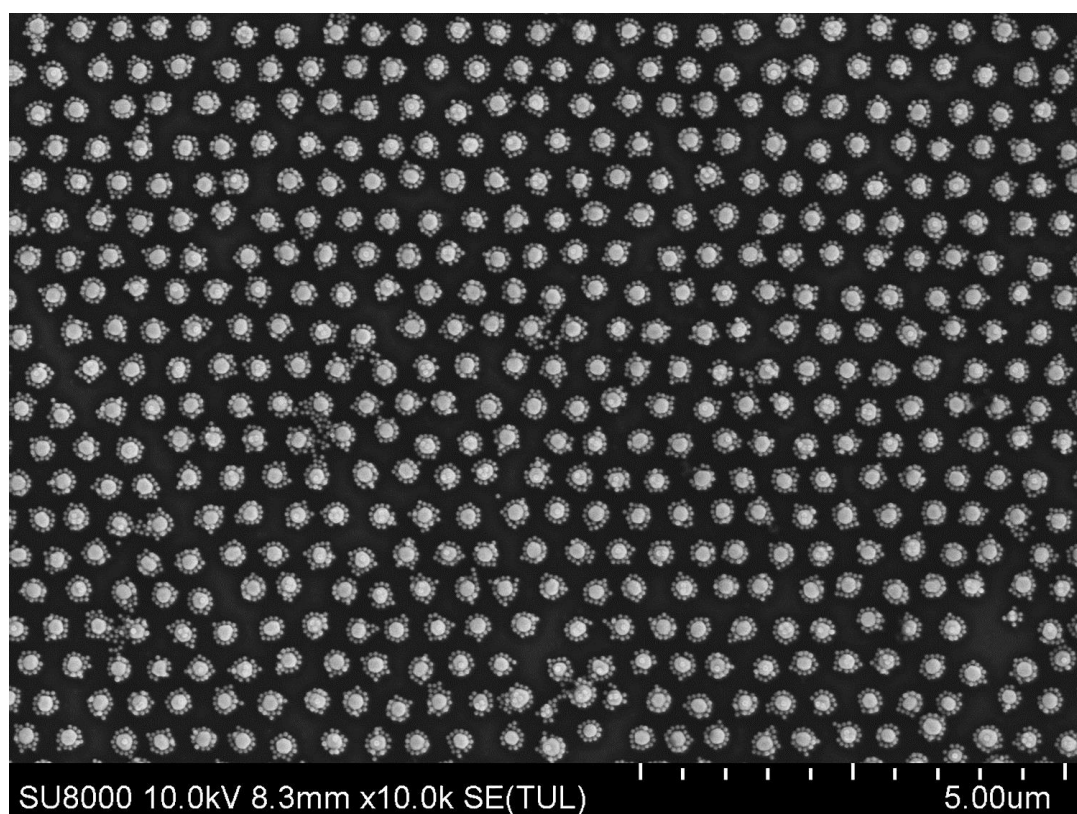


**Figure S8.** The SEM image of 2D NCP binary Au NP array with the satellite Au NP size of 55 nm.

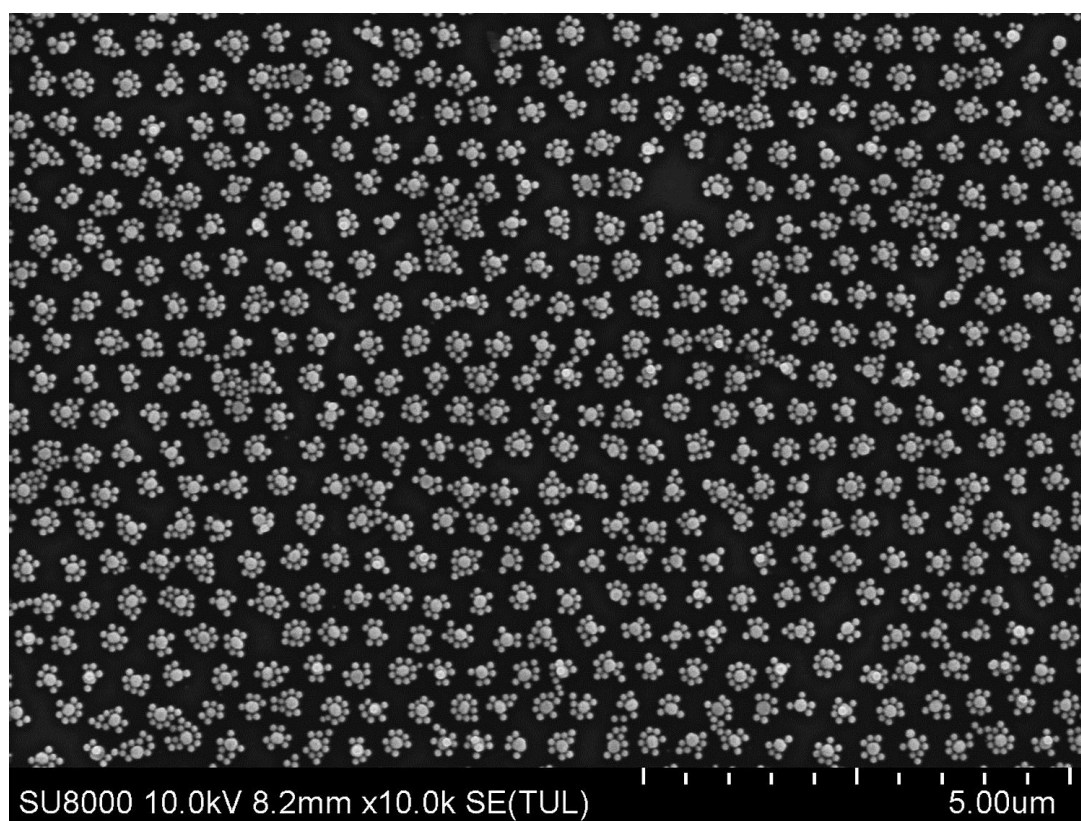


**Figure S9.** The SEM image of 2D NCP binary Au NP array with the satellite Au NP size of 85 nm.

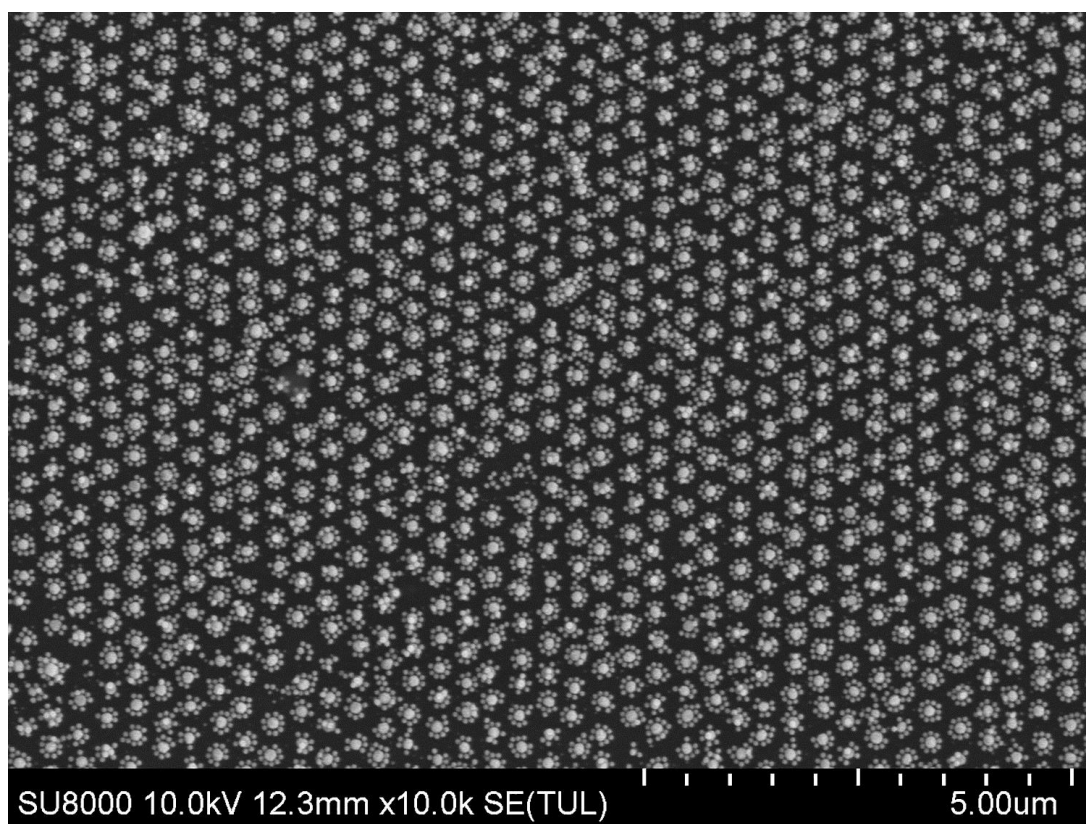


**Figure S10.** The SEM image of 2D NCP binary Au NP array with a period of 350 nm.

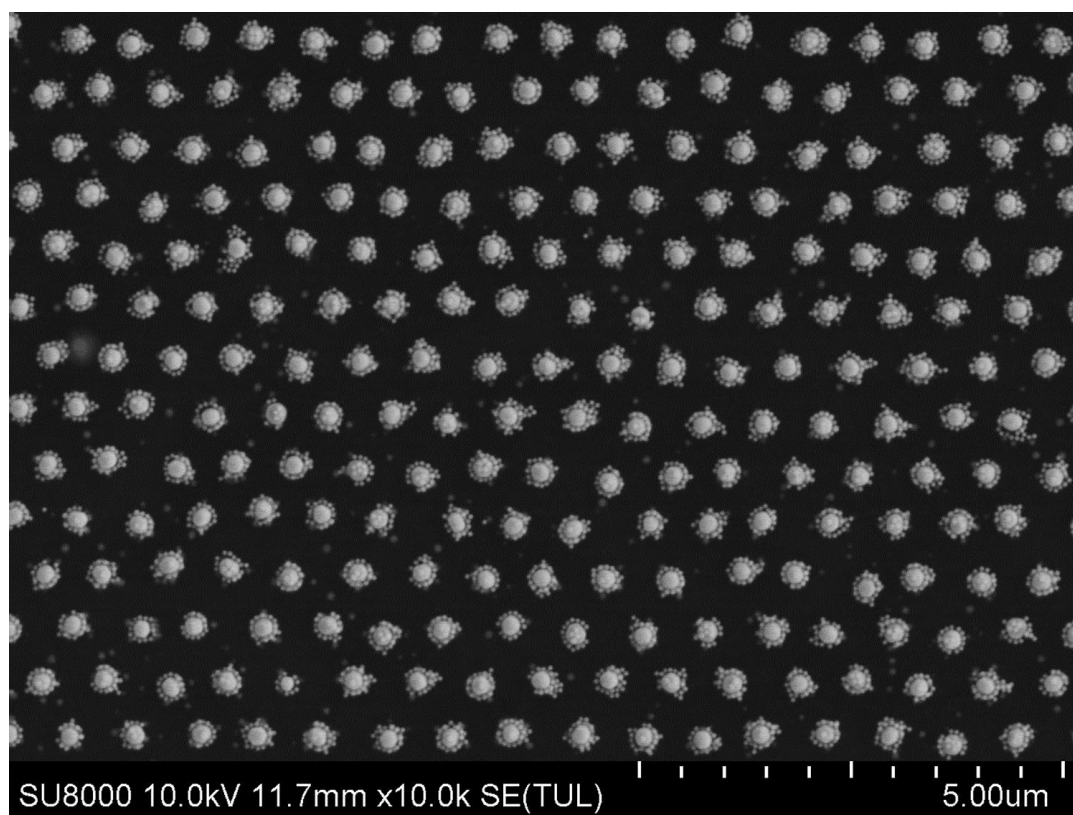


**Figure S11.** The SEM image of 2D NCP binary Au NP array with a period of 750 nm.

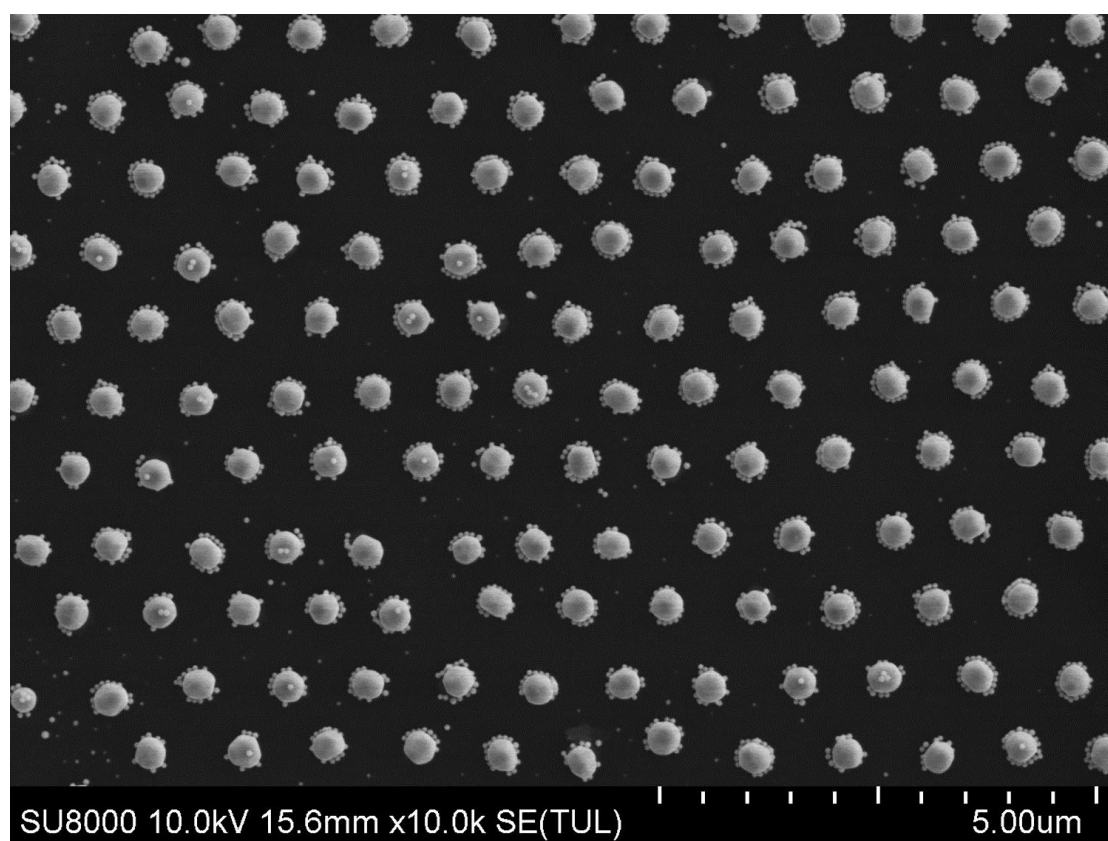


**Figure S12.** The SEM image of 2D NCP binary Au NP array with a period of 1000 nm.

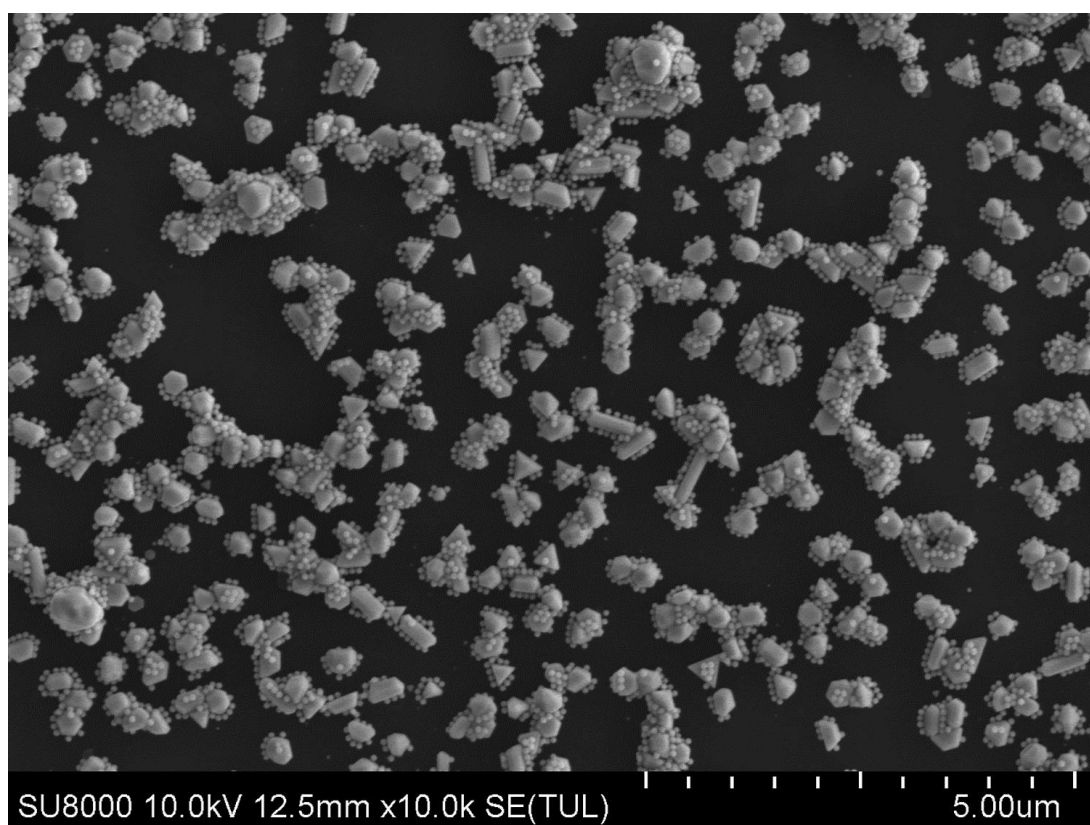


**Figure S13.** The SEM image of 'satellite' Au NPs assembled on a template randomly arranged with a series of irregular 'core' NPs.



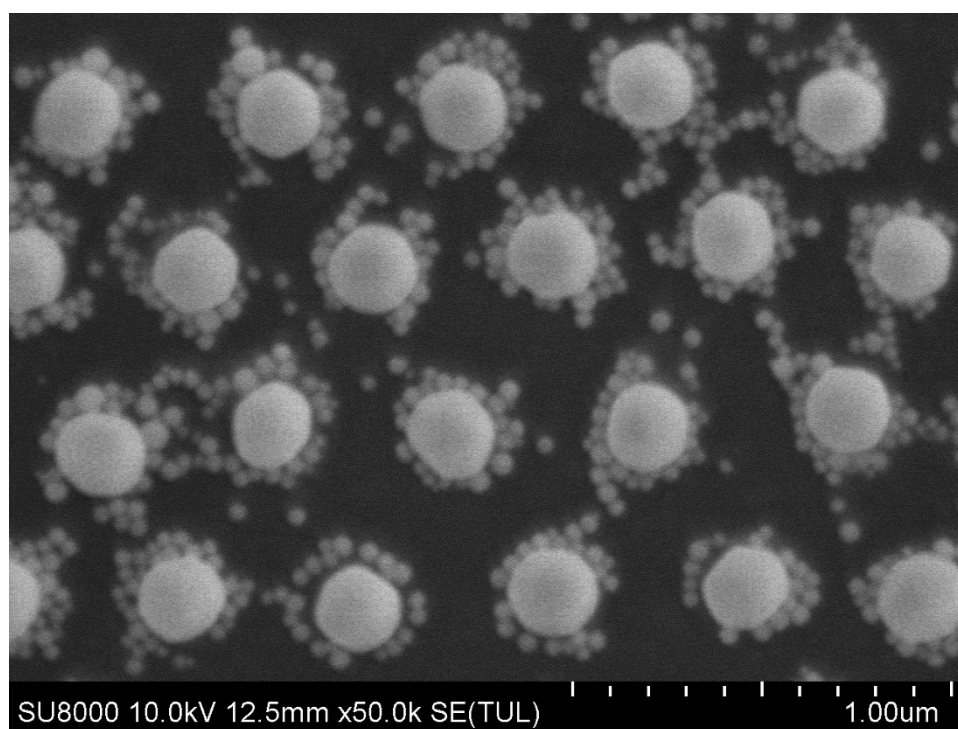


**Figure S14.** The SEM image of 2D NCP binary Au NP array with the PVP modified 'satellite' Au NPs.

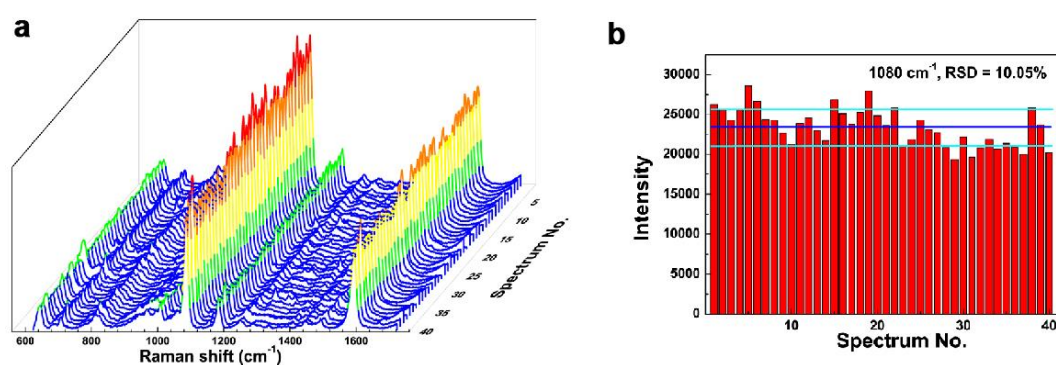


**Figure S15.** (a) The SERS spectra of 4-ATP molecules collected from five different NCP binary Au nanoparticle arrays with eight spectra per sample. (b) The analysis of intensity distribution of 1080  $\text{cm}^{-1}$  peak in (a). Note: RSD refers to the relative standard deviation. The 2D binary Au nanoparticle array demonstrates a low relative standard deviation of 10.05% in intensity.

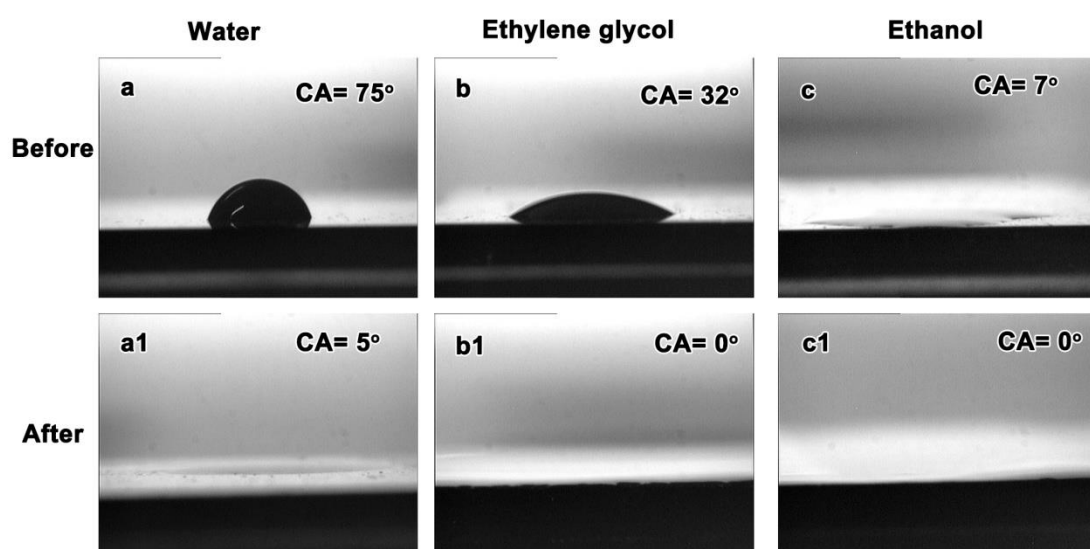


**Figure S16.** The Photographs of the contact angle (CA) of water (a, a<sub>1</sub>), ethylene glycol (b, b<sub>1</sub>), and ethanol (c, c<sub>1</sub>) solvents measured on the Si wafer substrate of 2D NCP unary Au nanoparticle before and after the hydrophilic treatment of UV-ozone cleaning.

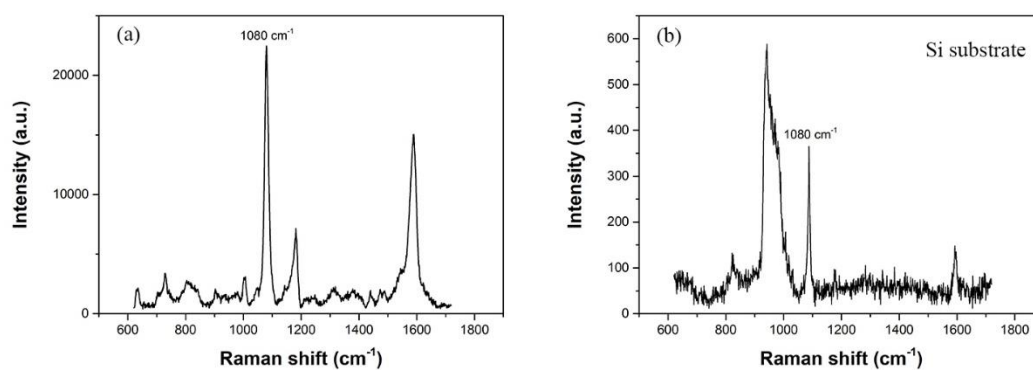


**Figure S17.** (a) The Raman spectra of 4-ATP molecules on 2D NCP binary Au nanoparticle array after dropping 5  $\mu\text{L}$  of  $10^{-6}$  M of 4-ATP ethanol solution. The surface area of the substrate of 2D NCP binary Au nanoparticle array is  $0.5 \times 0.5 \text{ cm}^2$ . (b) The Raman spectra of 4-ATP molecules on Si substrate after dropping 5  $\mu\text{L}$  of  $10^{-1}$  M of 4-ATP ethanol (the surface area of Si substrate is  $0.5 \times 0.5 \text{ cm}^2$ ).

## References

- (51) Lide, D. R. *CRC handbook of chemistry and physics*; CRC press: Boca Raton, FL, USA, 2004.
- (52) Kneipp, K.; Wang, Y.; Kneipp, H.; Perelman, L. T.; Itzkan, I.; Dasari, R. R.; Feld, M. S. Single molecule detection using surface-enhanced Raman scattering (SERS). *Phys. Rev. Lett.* **1997**, 78, 1667-1670.
- (53) Smallwood, I. *Handbook of organic solvent properties*; Butterworth-Heinemann: Oxford, UK, 2012.